Arch. Metall. Mater. **66** (2021), 1, 331-337

DOI: 10.24425/amm.2021.134791

J. TRZASKA[1*]

EXAMPLES OF SIMULATION OF THE ALLOYING ELEMENTS EFFECT ON AUSTENITE TRANSFORMATIONS DURING CONTINUOUS COOLING

The article shows examples of simulation of the chemical composition effect on austenite transformation during continuous cooling. The calculations used own neural model of CCT (Continuous Cooling Transformation) diagrams describing austenite transformations that occur during continuous cooling. The model allows to calculate a CCT diagrams of structural steels and engineering steels based on chemical composition of steel and austenitizing temperature. Examples of simulation shown herein are related to the effect of selected elements on the temperatures of phase transformations, hardness and volume fraction of ferrite, pearlite, bainite and martensite in steel.

Keywords: CCT diagram, simulation, neural network, heat treatment, steel

1. Introduction

Continuous Cooling Transformation (CCT) diagrams provide important information on the possibility of obtaining the required microstructure and hardness of steel depending on the process of its continuous cooling from the austenitizing temperature. They are useful while determining conditions of operation of heat treatment and thermo-mechanical treatment [1-3]. Frequently, parameters of phase transformation models are calculated based on CCT diagrams. Calculation of a CCT diagrams is an alternative for dilatometric and metallographic investigations. It reduces time needed to obtain results and costs of laboratory testing. Calculation of the CCT diagram can also be an introduction to laboratory investigations [4]. Various methods are used to model CCT diagrams [5-12]. The models presented in the literature can be used in various range of mass concentrations of elements. New work results are still being published in this regard [13-15].

Position and shape of austenite transformation curves on CCT diagrams depend mainly on chemical composition of steel, the starting condition of material and austenitizing conditions. Elements dissolved in a solid solution largely affect the kinetics of austenite transformation during cooling. The condition that needs to be fulfilled so that austenite chemical composition corresponds to the steel composition, is to dissolve carbides and other phases during austenitizing. Introducing several alloying elements into the steel makes that their impact is different than the total of individual impacts of elements added separately. Many times, not only the intensity but also trend of impact is changed. Analysis of effect of chemical composition on austenite transformations, including characteristics shown on CCT diagrams was a goal of multiple works. General trends are shown in guides and review articles, among others [1,16,17]. Detailed results for selected elements, transformations or steels, are shown in investigation and analysis reports [8,18-21].

Works [11,22] show a neural model of CCT diagram that allows to calculate a diagram for structural and engineering steels based on chemical composition and austenitizing temperature. The independent variables are mass concentrations of elements: C, Mn, Si, Cr, Ni, Mo, V, Cu, and austenitizing temperature. Artificial neural networks and data collection based on 550 CCT diagrams published in literature are used for modelling. CCT diagrams model is made of 17 artificial neural networks that solve classification and regression tasks.

Calculation process of CCT diagram is divided into two stages. At the first stage, it is verified if for the assumed cooling rate, the areas of ferrite, pearlite, bainite and martensite are present. For calculations, four neural classifiers are designed. The results allow to determine the range of cooling rate for each transformation. Upon considering classification results, temperatures at the beginning and end of transformations are calculated, as well as hardness and volume fractions of ferrite,

[1] SILESIAN UNIVERSITY OF TECHNOLOGY, DEPARTMENT OF ENGINEERING MATERIALS AND BIOMATERIALS, FACULTY OF MECHANICAL ENGINEERING, 18A KONARSKIEGO STR., 44-100 GLIWICE, POLAND

* Corresponding author: jacek.trzaska@polsl.pl

pearlite, bainite and martensite. The model is implemented in a CCT diagram calculation software. The model allows to simulate effect of selected elements on any temperature or time that describe austenite transformation as well as hardness and volume fraction of structural constituents that are formed due to steel cooling from austenitizing temperature. The article presents examples of simulation.

2. Method

Works [11,22] describe a CCT diagram model. The model describes the dependence between the steel chemical composition and austenitizing temperature and phase transformation temperature, hardness and volume fraction of structural constituents in a cooled steel continuously after austenitizing. CCT diagram model can be used to simulate impact of chemical composition, austenitizing temperature and cooling rate on CCT diagram or selected transformation temperature, hardness, volume fraction of structural constituents. Simulations can be done in range of mass concentrations of elements in which a CCT diagram model can be used. This range is shown in Table 1. Additional conditions that limit simulation are shown in Table 2.

Simulation of steel chemicalcompositionimpact can be done for:

- Pearlite into austenite transformation start temperature during heating Ac_1,
- Ferrite into austenite transformation finish temperature during heating Ac_3,
- Maximum temperature at which the austenite is transformed into bainite B_s
- Martensite start temperature M_s
- Temperature line of start austenite into ferrite transformation F_s,
- Temperature line of finish austenite into ferrite transformation F_f,
- Temperature line of start austenite into pearlite transformation P_s,
- Temperature line of finish austenite into pearlite transformation P_f,
- Temperature line of start austenite into bainite transformation $B_s(v_c)$,
- Temperature line of finish austenite into bainite transformation B_f,
- Temperature line of start austenite into martensite transformation $M_s(v_c)$,
- Hardness of steel cooled from austenitizing temperature,
- Volume fraction of: ferrite, pearlite, bainite and martensite in steel upon cooling from austenitizing temperature,
- Critical cooling rate,
- Time to start transformations.

The neural networks were evaluated based on the mean absolute error, Pearson correlation coefficient and the quotient of standard deviations. The quotient of standard deviations was calculated for the standard deviation of the forecast error and the standard deviation of the dependent variable. The quotient of standard deviations lets to relate an error made by model to the range of values of dependent variable. The best value of this statistic is equal to 0. Values of statistics calculated for the data from the verification set were compiled in Tables 3-5. The data from verification set were only used for numerical verification of neural networks.

TABLE 1

Ranges of mass concentrations of elements

	Mass fractions of elements, %								T_A,°C
	C	Mn	Si	Cr	Ni	Mo	V	Cu	
Min	0.1	0.28	0.13	0	0	0	0	0	780
Max	0.68	1.98	1.9	2.5	3.85	1.05	0.38	0.38	1050
T_A – austenitizing temperature, °C									

TABLE 2

Additional conditions for limiting the range of model application

	Mass fractions of elements, %			
	Mn+Cr	Mn+Cr+Ni	Cr+Ni	Mn+Ni
Max	3.6	5.6	5.3	4.5

TABLE 3

Statistic values used to evaluate the transformation temperature models (verification data set)

Transformation temperature	Mean absolute error,°C	Quotient of standard deviations	Correlation coefficient
Ac_1	10.4	0.36	0.76
Ac_3	12.1	0.22	0.91
B_s	19.4	0.25	0.89
M_s	13.4	0.16	0.97
F_s	16.0	0.25	0.93
F_f	19.0	0.33	0.87
P_s	15.4	0.32	0.88
P_f	20.4	0.32	0.87
$B_s(v_c)$	22.8	0.36	0.84
B_f	26.7	0.44	0.75
$M_s(v_c)$	13.6	0.17	0.97

TABLE 4

Statistic values used to evaluate the hardness model (verification data set)

	Mean absolute error, HV	Quotient of standard deviations	Correlation coefficient
Hardness	31.7	0.20	0.96

One of the ways to show simulation results is a graph that describes an impact of one or two independent variables on a value of a dependent variable. During calculations, it is necessary to determine constant values for independent variables that are not shown on the graph. The effect of chemical composition can be analyzed only in relation to concentrations of other elements. The values of other independent variables assumed during

TABLE 5

Statistic values used to evaluate model of the structural constituents (verification data set)

Structural constituent	Mean absolute error,%	Quotient of standard deviations	Correlation coefficient
Ferrite	5.8	0.30	0.93
Pearlite	4.9	0.27	0.95
Bainite	8.3	0.38	0.88
Martensite	4.9	0.24	0.96

simulation are especially important in the context of analysis of synergic impact of alloying elements on austenite transformations during cooling. The examples shown in the work assume such concentrations of elements to compare results with works of other authors.

3. Results

The article shows examples of simulation that can be done with CCT diagram model. Graphic presentation of results in the form of graphs are shown in Figures 1-5.

Figure 1 shows examples of simulated effect of chemical composition of steel on temperature B_s. Two levels of concentrations of other elements are assumed. In the presented results, B_s is the temperature above which bainite is not formed even in isothermal conditions.

Simulation results (Fig. 1) confirm the impact of elements on the B_s temperature shown in many empirical equations. The equations are collected, among others, in the works [11,23]. Most of them have a linear form. Impact of element on the temperature is shown by the value of regression coefficient that does not change within the whole range of equation. The equations do not take into account the relations between the element on the transformation temperature and mass concentration of other elements. Based on a regression coefficient, it can be estimated how much the transformation temperature will change with the change of element concentration by 1%. Empirical equations differ in range of values of independent variables for which they can be used. Equation coefficient are calculated based on different datasets by analyzing the impact of chemical composition on temperature B_s for different groups of steel. The value of the regression coefficient is affected by the range of element concentration and the distribution of its values in the data set collected for calculations.

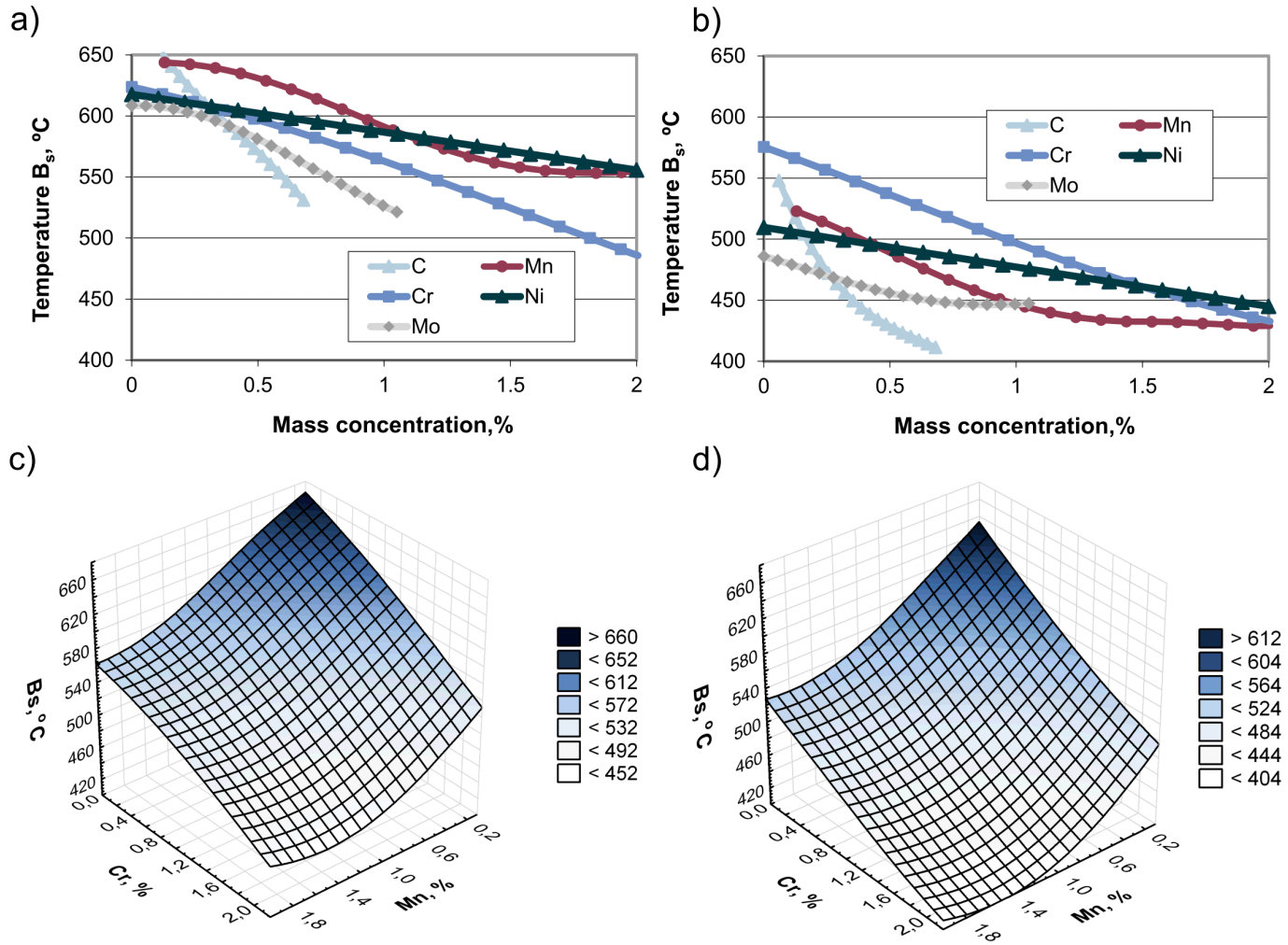

Fig. 1. Simulation of the effect of alloying elements on the B_s temperature of the steel with concentrations: a) and c) 0.3%C, 0.8%Mn, 0.4%Si, 0.3%Cr, 0.3%Ni, 0.05%Mo; b) and d) 0.3%C, 0.8%Mn, 0.4%Si, 1.5%Cr, 1.5%Ni, 0.4%Mo

In all the equations, the highest impact of carbon is shown. Sequence of impact of other elements considered in Figure 1 is not always the same. Just as in the example on the figure, in most equations, right after carbon, manganese and molybdenum are indicated, then chromium and nickel. Non-linear impact of manganese and molybdenum and carbon can be noted for higher concentrations of other elements. The effect of molybdenum on the B_s temperature decreases for higher contents of other alloying elements. It is seen that this decrease mainly occurs for contents higher than 0.50% Mo. Non-linear carbon impact is defined by Van Bohemen in his formula [24]. The complex impact of manganese, nickel molybdenum and chromium is pointed by Lee in its formula [25]. These conclusions are confirmed by simulation results showing impact of two independent variables. Figures 1c and 1d show examples of chromium and manganese impact on B_s temperature. A change of manganese impact can be noted depending on chromium concentration and concentrations of other alloying elements. The effect of manganese on the B_s temperature decreases above a content of about 1% of this element. This effect is clearly visible for higher contents of other alloying elements. Discussion on the impact of steel chemical composition on B_s temperature supported by results of investigations for model alloys and commercial steels are shown in work [18]. Increasing concentrations of elements that reduce B_s temperature in the steel contributes to the formation of the lower bainite which is beneficial due to the higher crack resistant. Also, the same elements clearly reduce M_s temperature which contributes to the higher risk of quench cracks.

Figure 2 shows examples of simulated impact of steel chemical composition on M_s temperature. Just as for B_s temperature, two concentrations levels of other elements are assumed.

The results show that carbon is the element that reduces M_s temperature the most. Manganese impact is greater with the increased concentrations of other elements such as chromium, nickel or molybdenum. A similar impact of molybdenum can be noted as well. Impact of other elements considered in calculations is similar. Similar conclusions are drawn after analyzing regression coefficients of empirical equations [11,23]. Non-linear carbon impact is pointed by Van Bohemen [24] and Andrews [26], who also notes synergic impact of carbon and manganese as well as carbon and chromium. Andrews conclusions confirm simulation results of carbon and manganese impact shown in Figures 2c and 2d. Non-linear carbon impact is especially visible with low concentration of manganese and other alloying elements.

Figure 3 shows simulation of carbon effect on CCT diagrams by varying the carbon content from 0.22 to 0.50% for steel which contain 0.65% Mn, 0.25% Si, 1% Cr, 0.1% Ni and 0.15%

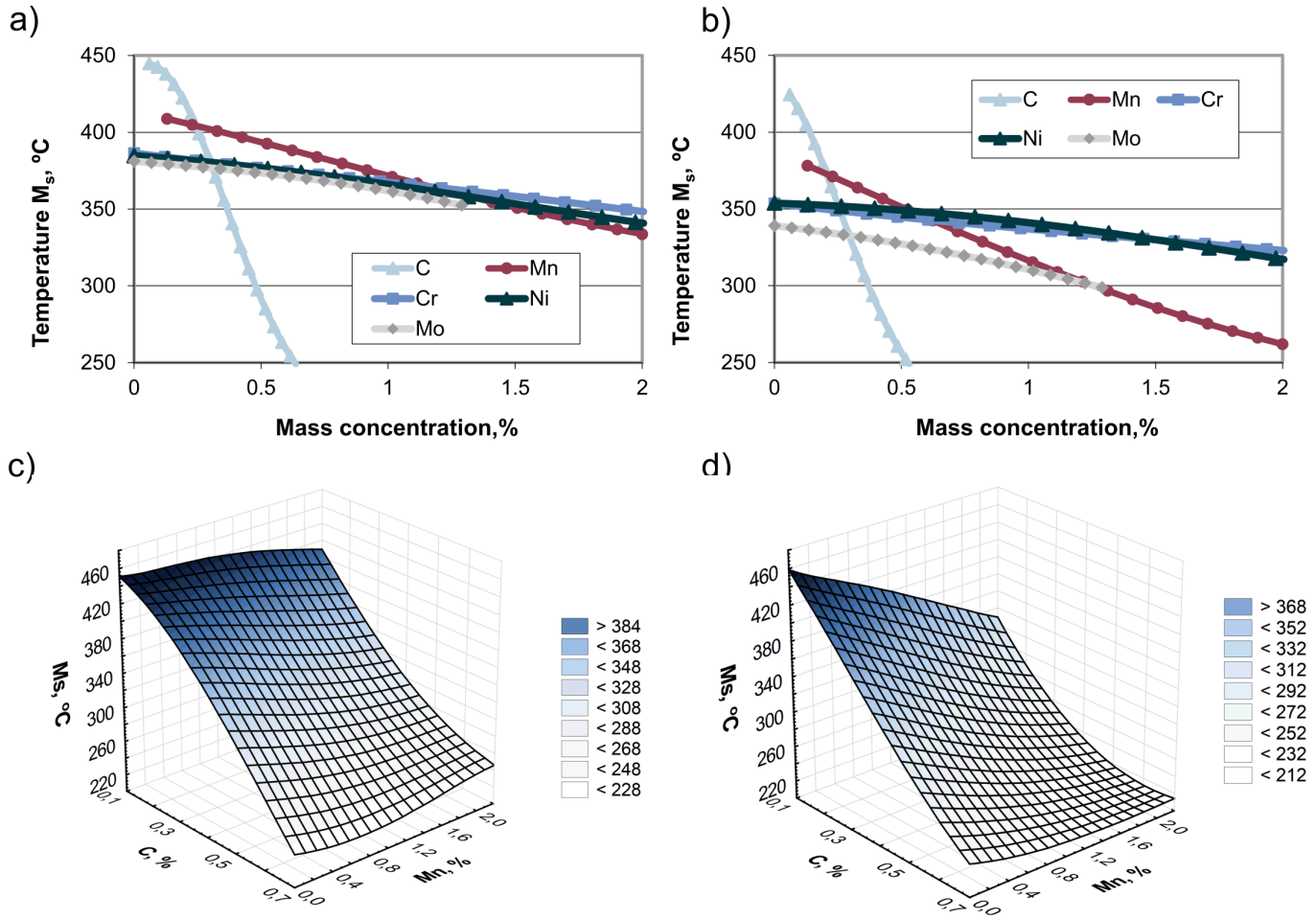

Fig. 2. Simulation of the effect of alloying elements on the M_s temperature of the steel with concentrations: a) and c) 0.3%C, 0.8%Mn, 0.4%Si, 0.3%Cr, 0.3%Ni, 0.05%Mo; b) and d) 0.3%C, 0.8%Mn, 0.4%Si, 1.5%Cr, 1.5%Ni, 0.4%Mo

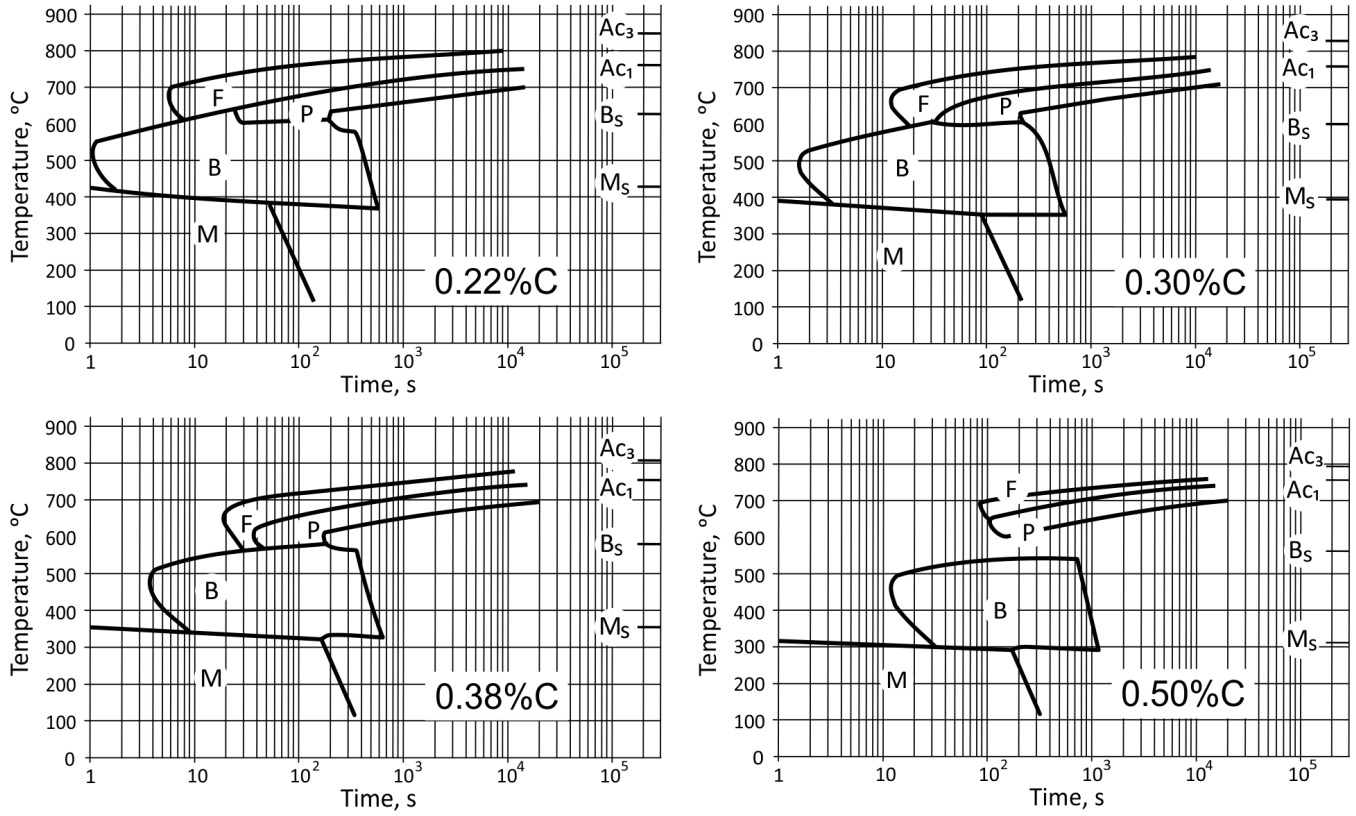

Fig. 3. Simulation of the effect of carbon on the CCT diagram of the steel with concentrations: 0.65%Mn, 0.25%Si, 1%Cr, 0.1%Ni, 0.15%Mo, austenitised at temperature of 850°C

Mo, with an austenitizing temperature 850ºC. Higher carbon concentration clearly contributes to the longer time needed to start transformations austenite into ferrite as well as austenite into bainite. Time needed to begin pearlite transformation is slightly changed. The shift of the pearlite region to lower cooling rates occurs for content higher than 0.30% of carbon. The ferrite region reduces in size with increasing carbon concentration. Lines describing beginning of bainitic and martensitic transformations are displaced towards lower temperature. The ferrite start temperature is affected by carbon content, especially for low cooling rates. Temperature of start the pearlite transformation is affected less by the carbon content. Increasing the carbon content to about 0.5% causes that the pearlite and bainite regions are separated by an austenite. The results confirm the experimental graphs shown in [16]. Similar results are described based on investigations of steel and model alloys in the work [18].

Figure 4 shows examples of simulation of chromium and manganese effect on hardness of steel with base composition 0.25% C, 0.25% Si, 0.75% Mn, cooled continuously from austenitizing temperature. The addition of chromium does not increase the maximum hardness. Increasing the chromium concentration to about 1.5% increases the hardenability of the

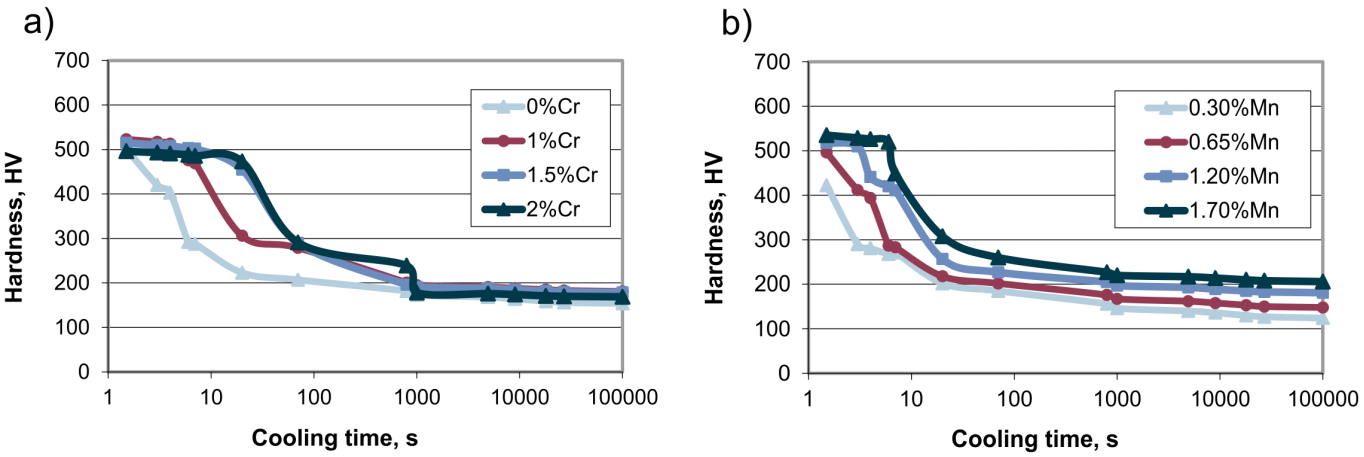

Fig. 4. Simulation of the effect of chromium (a) and manganese (b) on the hardness of the steel with concentrations: 0.25%C, 0.25%Si, 0.75%Mn (a), 0%Cr (b), austenitised at temperature of 900°C

steel. This may be partly due to the basic chemical composition of the steel selected for simulation. In this simulation, chromium is added to steel also containing 0.75% manganese. The combined effects of these alloying elements cause an additional increase in hardenability. The hardness curve correspond with the volume fractions of structural constituents shown in Figure 5. High hardness occurs where high volume fractions of martensite develop. At long cooling times, the addition of chromium does not significantly affect the hardness of steel. In this case, the microstructural constituents are only ferrite and pearlite. The addition of manganese increase the maximum hardness and increases the hardenability. Increasing the maximum hardness occurs for content to about 0.65% of manganese. Manganese significantly increases hardness at high cooling rates, but has little effect on the hardness at low cooling rates.

Figure 5 shows volume fractions changes of ferrite, pearlite, bainite and martensite as a function of cooling time and depending on chromium concentration, for steels which further contain 0.25% C, 0.75% Mn and 0.25% Si, with an austenitizing temperature 900°C. At long cooling time chromium addition increases the volume fraction of pearlite as well as reduces the volume fraction of ferrite. Chromium addition increases the incubation time of bainite, consequently bainite is formed at longer cooling times. The addition of chromium increases the volume fraction of bainite, but the model error (Table 5) does not allow this conclusion to be confirmed. Increasing the concentration of chromium extends the cooling time in which the martensitic transformation occurs. Similar simulation results are shown in the work [8].

4. Summary

The article presents examples of simulated impact of steel chemical composition on phase transformation temperatures, hardness and volume fractions of structural constituents in the steel cooled from austenitizing temperature. Neural model of CCT diagrams described in works [11,22] is used for calculations.

Analysis of impact of an element on the steel properties shown in CCT diagrams requires determination of concentrations of other elements. It is necessary to produce model alloys and many research experiments. Tests are expensive and time-consuming. The analysis makes it difficult for synergic impact of alloying elements. The addition of several alloying elements into the steel makes that their impact is different than the total impacts of individual elements added separately. Having an adequate model allows to perform initial numeric experiments and/or reduce total number of experiments. This reduces the costs and testing time [11,27-29].

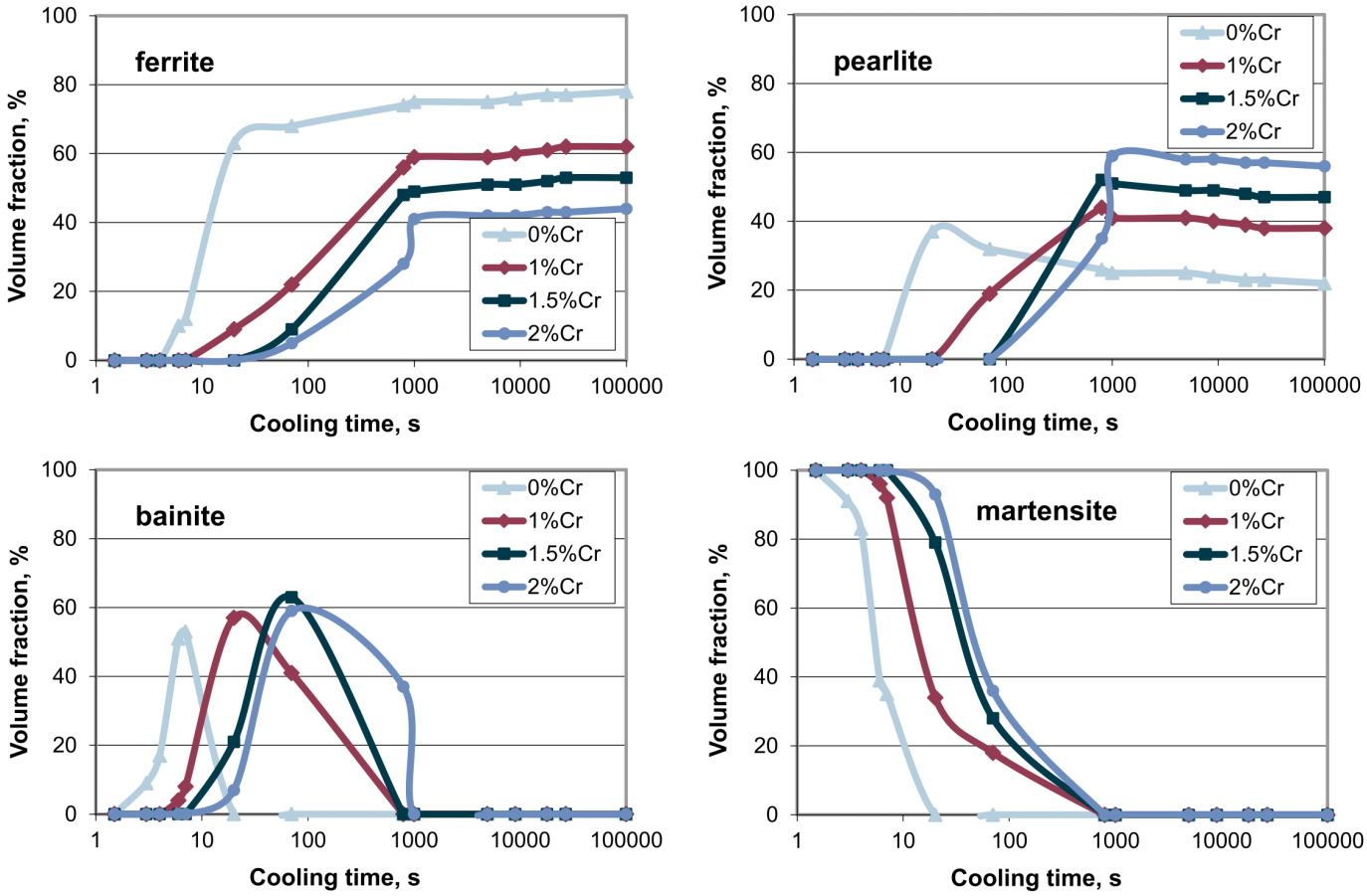

Fig. 5. Simulation of the effect of chromium on the ferrite, pearlite, bainite and martensite fractions in steel with concentrations: 0.25%C, 0.25%Si, 0.75%Mn, austenitised at temperature of 900°C

Most of the empirical equations published in the literature assume linear impact of alloying elements. The force of this impact is a described value of regression coefficient. This simplification comes down to estimating temperature of phase transformation. However, it makes it difficult to analyze the effect of alloying elements on the transformation temperature. This issue in the neural model is non-existent. Unfortunately, there is a risk of overfitting of the model to the data from the training set. Overfitting of neural networks is a rather frequent case. In this case, the graphs showing simulation results may have areas resulting from overfitting and not synergic impact of alloying elements.

Given the errors that are always related to modelling, simulation calculations should be partially confirmed with laboratory tests. In many cases, it is possible with the results of tests of commercial steels and model alloys that are published in the literature. The model errors should be also born in mind when analyzing simulation results. Small, as compared to the value of error, changes of values shown in the graph may be not caused by actual effect of an element. They may arise only from calculation errors.

Acknowledgements

This publication was financed by the Ministry of Science and Higher Education of Poland as the statutory financial grant of the Faculty of Mechanical Engineering SUT.

REFERENCES

[1] J.C. Zhao, M.R. Notis, Mater. Sci. Eng. **15**, 135-207 (1995).

[2] M. Opiela, B. Grzegorczyk, Thermo-mechanical treatment of forged products of Ti-V-B microalloyed steel, Metal'2013 Conference Proceedings, Brno (2013).

[3] A. Grajcar, M. Opiela, Arch. Mater. Sci. Eng. **32** (1), 13-16 (2008).

[4] A. Grajcar, M. Morawiec, W. Zalecki, Metals **8**, 1028-1039 (2018), DOI:10.3390/met8121028.

[5] J. Trzaska, A. Jagiełło, L.A. Dobrzański, Arch. Mater. Sci. Eng. **39**, 13-20 (2009).

[6] V. Colla, M. Desanctis, A. Dimatteo et al., Metall. and Mat. Trans. A **42**, 2781-2793 (2011), DOI:10.1007/s11661-011-0702-3.

[7] C. Capdevila, Neural networks modeling of phase transformations in steels, in: E. Pereloma, D.V. Edmonds (Eds.) Phase Transformations in Steels, Woodhead Publishing (2012), DOI: 10.1533/9780857096111.3.464.

[8] P.J. Van der Wolk, Modelling CCT-Diagrams of Engineering Steels Using Neural Networks, Delft University Press, Delft (2001).

[9] F. Nurnberger, M. Schaper, F.W. Bach, J. Mozgova, K. Kuznetsov, A. Halikova, O. Perederieieva, Adv. Mater. Sci. Eng. **1**, 1-10 (2009), DOI: 10.1155/2009/582739.

[10] N Saunders, Z. Guo, X. Li, A.P. Miodownik, J.P Schillé. JOM **55** (12), 60-65 (2003).

[11] J. Trzaska, Prediction methodology for the anisothermal phase transformation curves of the structural and engineering steels, Silesian University of Technology Press, Gliwice (2017), (in Polish).

[12] N. Isasti, P.M. Garcia-Riesco, D. Jorge-Badiola, M. Taheri, B. Lopez, P. Uranga, ISIJ Int. **55** (9), 1963-1972 (2015), DOI: 10.2355/isijinternational.ISIJINT-2015-036.

[13] X. Geng, H. Wang, W. Xue, S. Xiang, H. Huang, L. Meng, G. Ma, Comp Mater Sci **171**, (2020), DOI: 10.1016/j.commatsci. 2019.109235 (in press).

[14] S. Chakraborty, P.P. Chattopadhyay, S.K. Ghosh, S. Datta, Appl. Soft. Comput. **58**, 297-306 (2017), DOI: 10.1016/j.asoc.2017. 05.001.

[15] M. Rahaman, W. Mu, J. Odqvist, P. Hedstrom, Metall. Mater. Trans. A **50A**, 2082-2091 (2019), DOI: 10.1007/s11661-019-05170-8.

[16] G.F. Vander Voort (Ed.), Atlas of Time-Temperature Diagrams for Irons and Steels, ASM International (2004).

[17] G.E. Totten, M.A.H. Howes (Eds.), Steel Heat Treatment Handbook, Marcel Dekker Inc., New York (1997).

[18] J. Pacyna, Chemical composition and steel structures design, AGH Publishers, Cracow (1997) (in Polish).

[19] J. Wang, P.J. Van Der Wolk, S. Van Der Zwaag, ISIJ Int. **39**, 1038-1046 (1999).

[20] J. Zhao, Z. Jiang, J. Soo. Kim, C. Soo. Lee, Mater. Design **49**, 252-258 (2013), DOI: 10.1016/j.matdes.2013.01.056.

[21] B. Pawłowski, P. Bała, R. Dziurka, the effect of alloying elements on the temperature range of pearlite to austenite transformation in low alloy hypoeutectoid steels, Metal'2013 Conference Proceedings, Brno (2015).

[22] J. Trzaska, Arch. Metall. Mater. **63** (4), 2009-2015 (2018), DOI: 10.24425/amm.2018.125137.

[23] A.A. Gorni, Steel Forming And Heat Treating Handbook, www.gorni.eng.br/e/Gorni_SFHTHandbook.pdf, accessed: 23.10.2019

[24] S.M.C. Van Bohemen, J. Mater. Sci. Technol. **28** (4), 487-495 (2012), DOI: 10.1179/1743284711Y.0000000097.

[25] Y.K. Lee, J. Mater. Sci. Lett. **21** (16), 1253-1255 (2002).

[26] K.W. Andrews, Journal of the Iron and Steel Institute **203**, 721-727 (1965).

[27] W. Sitek, Trans. Famena 34 (3), 39-46 (2010).

[28] L.A. Dobrzański, T. Tański, J. Trzaska, Mater. Sci. Forum 638, 1498-1493 (2010), DOI:10.4028/www.scientific.net/MSF.638-642.1488.

[29] B. Smoljan, D. Iljkić, L. Pomenić, Int. J. Microstruct. Mater. Prop. **8** (1/2), 97-112 (2013).